

Stokes' drift: a rocking ratchet

I. Bena, M. Copelli and C. Van den Broeck

Limburgs Universitair Centrum
B-3590 Diepenbeek, Belgium

December 4, 2017

Abstract

We derive the explicit analytic expression for the Stokes' drift in one dimension in the presence of a dichotomic Markov forcing. For small amplitudes of the forcing, the drift is enhanced, but the enhancement is reduced with increasing frequency of the forcing. On the other hand, a reduction of the drift or even a flux reversal can be induced at larger amplitudes, while the flux is now found to be an increasing function of the perturbation frequency.

PACS numbers: 02.50.-r, 05.40.+j, 05.60.+w

1 Introduction

A longitudinal wave travelling through a fluid imparts a net drift motion to the suspended particles - an effect known as *Stokes' drift*. The *classical* Stokes' drift [1] refers only to the deterministic behavior, i.e. it does not account for the stochastic fluctuations or perturbations in the system. It has been extensively studied in various practical contexts like, for instance, the motion of tracers in meteorology and oceanography [2] and that of the (doping) impurities in crystal growth [3]. A simple intuitive explanation of classical Stokes' drift is that the suspended particles spend a longer time in the regions of the wave-train where the force due to the wave acts in the direction of wave's propagation than the time spent in those regions where the force acts in the opposite direction; therefore particles are driven in the sense of wave's propagation. When several linearly superposed waves are present, the resulting drift velocity is simply the sum of the contributions from each wave [4].

Recently, there has been some interest in *stochastic* Stokes' drift ([4, 5, 6], see also [7]). It was found that the diffusive motion of the suspended particles can significantly alter the amplitude of the drift velocity. But it is the merit of [5] to open stochastic Stokes' drift to further investigation by putting it in its natural context, namely *ratchet-like Brownian motors* in which the thermal motion of small (microscopic) particles is rectified by an asymmetric time-dependent potential [8]. This scenario is referred to as the *flashing ratchet*. Paper [5] is limited to the case when the motion of the overdamped suspended particles is diffusion-dominated, i.e. when the deterministic forcing due to the wave is very weak. An approximate perturbative technique is developed for calculating the

drift velocity in arbitrary dimensions, which shows that the drift depends on particles' diffusivity in magnitude and, in more than 1D, also in direction (a very appealing feature, useful in particle selection devices - see, for example, in [9] Doering et al, 1994, and in [8] M. Bier, 1996). Papers [6] and, in a very different context [7], give an exact integral expression for Stokes' drift of overdamped diffusive particles in 1D, for arbitrary wave forms. Using a Fokker-Planck equation technique, it finds that white noise reduces Stokes' drift by comparison to its classical (deterministic) value, the flux reversal being absent.

The purpose of this short communication is to show that the characteristics of the 1D Stokes' drift may become more complex (including flux reversal or enhancement of the classical drift) when the particles are subjected to stochastic forcing that is non-white (i.e. it has a finite correlation time). We will focus on the case of dichotomic Markov forcing, in which the particle is subjected to a randomly alternating force, in addition to the force exerted by the wave. For this choice of coloured noise, explicit analytic results can be obtained, while this is not the case for other types of coloured noise, including the Ornstein-Uhlenbeck process. Even though the time-average of the dichotomic force is taken to be zero, its effect in conjunction with the asymmetry of the wave's perturbation is highly nontrivial. As such the model realizes in the Stokes' drift context another paradigm of Brownian motors, namely that of the so-called *rocking ratchet*. In this scenario, the systematic motion acquired under influence of an alternating zero-average force essentially revolves on the asymmetry of the nonlinear response in the presence of a steady but asymmetric potential [9]. The dichotomic Markov forcing presents another important advantage in that the exact integral expression for Stokes' drift can be derived. Furthermore, in some cases of interest, the resulting integrals can be evaluated explicitly. Our analytic results are also complemented with computer simulations, which are found to be in full agreement with the theory.

2 The model

The starting point is the following stochastic differential equation:

$$\dot{X}_t = f(X_t - vt) + \xi(t) , \quad (1)$$

where $\xi(t)$ is a symmetric dichotomic noise (a two-step Markov process) [10]. It can take only two values, $\pm A$, with equal probability, jumping between them with a probability k per unit time. It has zero mean and its autocorrelation function $\langle \xi(t) \xi(t') \rangle = A^2 \exp(-2k|t - t'|)$ shows a finite correlation time $\tau_c = 1/2k$.

With a suitable time scaling, eq.(1) models the 1D overdamped motion of a Brownian particle subjected to a dichotomic forcing. X_t is the particle position at time t , while f is the periodic forcing due to the wave travelling at the speed v with wavelength λ :

$$f(y + \lambda) = f(y) , \forall y , \quad (2)$$

with $f(y) < v , \forall y$ as the case of physical relevance.

The quantity of interest is the *drift velocity*, which represents the mean velocity of the particles in the long time limit:

$$\vartheta = \lim_{t \rightarrow \infty} \frac{1}{t} \langle X_t \rangle , \quad (3)$$

where the mean is to be taken over the realisations of the dichotomic noise. By defining a new variable $Y_t = X_t - vt$ one can rewrite eq.(1) as:

$$\dot{Y}_t = F(Y_t) + \xi(t) , \quad (4)$$

with $F(y) \equiv f(y) - v$, and therefore:

$$\begin{aligned} \vartheta - v &= \lim_{t \rightarrow \infty} \frac{1}{t} \langle Y_t \rangle \\ &= \lim_{t \rightarrow \infty} \int_{-\infty}^{+\infty} dy F(y) [\rho_+(y, t) + \rho_-(y, t)] . \end{aligned} \quad (5)$$

Here $\rho_{\pm}(y, t)$ represent the probability densities for the particle position y and the value of the dichotomic noise equal to $\pm A$, respectively. Their time evolution is described by [10]:

$$\begin{aligned} \frac{\partial \rho_+(y, t)}{\partial t} &= -\frac{\partial}{\partial y} [(F + A)\rho_+] - k(\rho_+ - \rho_-), \\ \frac{\partial \rho_-(y, t)}{\partial t} &= -\frac{\partial}{\partial y} [(F - A)\rho_-] - k(\rho_- - \rho_+). \end{aligned} \quad (6)$$

The first term in the r.h.s. of each of these equations corresponds to the deterministic flow in phase space (between two jumps of the dichotomic noise), while the other term corresponds to the jumps of the dichotomic noise between $\pm A$. Because of the periodicity (2) of $f(y)$ ($F(y)$), in order to evaluate (5) we only need to study the asymptotic behavior of the reduced probability density:

$$P(y, t) = \sum_{n=-\infty}^{\infty} [\rho_+(y + n\lambda, t) + \rho_-(y + n\lambda, t)] . \quad (7)$$

From its definition, it is obvious that the reduced probability density is subjected to periodic boundary conditions:

$$P(y + \lambda, t) = P(y, t) , \quad \forall y, t, \quad (8)$$

while the normalization condition reads:

$$\int_0^{\lambda} P(y, t) dy = 1. \quad (9)$$

Considering also the quantity

$$p(y, t) = \sum_{n=-\infty}^{+\infty} [\rho_+(y + n\lambda, t) - \rho_-(y + n\lambda, t)] , \quad (10)$$

it follows from (6) that $P(y, t)$ and $p(y, t)$ obey a set of coupled evolution equations:

$$\begin{aligned} \frac{\partial P(y, t)}{\partial t} &= -\frac{\partial}{\partial y} (FP) - A \frac{\partial}{\partial y} p, \\ \frac{\partial p(y, t)}{\partial t} &= -\frac{\partial}{\partial y} (Fp) - A \frac{\partial}{\partial y} P - 2kp. \end{aligned} \quad (11)$$

The stationary solution $P^{st}(y)$ can be easily found [11]:

$$P^{st}(y) = \frac{1}{Z} \int_y^{y+\lambda} \frac{F'(y') + 2k}{F^2(y') - A^2} \exp[-\phi(y') + \phi(y)] dy', \quad (12)$$

which is valid as long as $F^2(y) - A^2 \neq 0, \forall y$. Here $\phi(y)$ is defined by:

$$\phi(y) = -2 \int_0^y \frac{F(y')[F'(y') + k]}{F^2(y') - A^2} dy'. \quad (13)$$

and Z is the normalization factor according to eq.(9). Therefore the drift velocity can be finally expressed as:

$$v = \int_0^\lambda f(y) P^{st}(y) dy. \quad (14)$$

These results are valid for an arbitrary wave form, provided that the obvious necessary differentiability and integrability conditions are fulfilled. Note that the drift depends nonlinearly on F , so that the contributions of different waves are not additive.

3 The piecewise linear wave

An explicit analytical expression for $P^{st}(y)$ can be obtained in the case of a piecewise linear wave forcing:

$$F(y) = \begin{cases} -(1-b)v, & y \in [0, \lambda/2 - 2\varepsilon[\bmod \lambda \\ -[(1-b)v + bv(y - \lambda/2 + 2\varepsilon)/\varepsilon], & y \in [\lambda/2 - 2\varepsilon, \lambda/2[\bmod \lambda \\ -(1+b)v, & y \in [\lambda/2, \lambda - 2\varepsilon[\bmod \lambda \\ -[(1+b)v - bv(y - \lambda + 2\varepsilon)/\varepsilon], & y \in [\lambda - 2\varepsilon, \lambda[\bmod \lambda, \end{cases} \quad (15)$$

with $0 < b < 1$. A square wave corresponds to $\varepsilon \rightarrow 0$, while $\varepsilon = \lambda/4$ represents the triangular-like wave.

The final expressions for $P^{st}(y)$ are rather lengthy and will not be reproduced here. But we performed numerical simulations, which show very good agreement with theoretical results, cf. fig. (1). Note that these results are valid for $0 < A < (1-b)v$ or for $A > (1+b)v$.

The analytic results for the square-like wave, corresponding to the limit $\varepsilon \rightarrow 0$, are of more interest. They read as follows:

$$P^{st}(y) = Z^{-1} \left\{ \frac{1 - e^{-U-V}}{(1-b)v} + \frac{e^{2Uy/\lambda}}{(1-b^2)v} [e^{-U} - e^{-U-V}] \frac{2A^2b}{(1-b)^2v^2 - A^2} \right\}, \quad (16)$$

for $y \in [0, \lambda/2[$, and

$$P^{st}(y) = Z^{-1} \left\{ \frac{1 - e^{-U-V}}{(1+b)v} - \frac{e^{V(2y/\lambda-1)}}{(1-b^2)v} [e^{-V} - e^{-U-V}] \frac{2A^2b}{(1+b)^2v^2 - A^2} \right\}, \quad (17)$$

for $y \in [\lambda/2, \lambda[$, where we introduced the dimensionless variables:

$$\begin{aligned} U &\equiv \frac{\alpha(1-b)}{2[(1-b)^2\beta^2-1]}, \\ V &\equiv \frac{\alpha(1+b)}{2[(1+b)^2\beta^2-1]}, \\ \alpha &\equiv \frac{2kv\lambda}{A^2}, \quad \beta \equiv \frac{v}{A} \end{aligned} \tag{18}$$

The following expression for the drift velocity is obtained:

$$\frac{\vartheta}{\vartheta_{cl}} = \frac{1 - e^{U+V} - \frac{4}{(1-b^2)\alpha}(1 + e^{U+V} - e^U - e^V)}{1 - e^{U+V} - \frac{4b^2}{(1-b^2)\alpha}(1 + e^{U+V} - e^U - e^V)}, \tag{19}$$

where $\vartheta_{cl} = b^2v$ is the classical value of the Stokes' drift velocity. We mention some limiting cases of interest. First, the limit $A \rightarrow 0$ or $k \rightarrow \infty$ (i.e. $\beta \rightarrow \infty$ and/or $\alpha \rightarrow \infty$) leads to the classical value of the Stokes' velocity $\vartheta/\vartheta_{cl} = 1$. Second, the drift velocity derived in [6] is recovered in the white noise limit $A \rightarrow \infty$, $k \rightarrow \infty$, with $A^2/2k = D$ finite ($\beta \rightarrow 0$). Finally, the quenched-noise limit $k \rightarrow 0$ ($\alpha \rightarrow 0$) (i.e. half of the particles, chosen at random, are subjected to a constant external forcing $+A$, while the other half to an external forcing $-A$) results in the following mean velocity:

$$\frac{\vartheta_{qn}}{\vartheta_{cl}} = \frac{\beta^2}{\beta^2 - 1}. \tag{20}$$

This expression reveals the possibility of a *flux reversal*: the drift velocity is negative for $\beta < 1$, i.e. for sufficiently large amplitude.

Turning to the general case, we have represented in Fig. 2 the results of eq. (19) together with simulations for the square wave for two representative sets of parameter values. For small values of the forcing amplitude A one finds that the drift is enhanced ($\vartheta/\vartheta_{cl} > 1$), but the enhancement is reduced upon increasing the frequency of the perturbation. In fact one can prove that enhancement occurs whenever $A < (1-b)v$, by noting that $U, V > 0$ and making use of the inequality $e^x \geq 1+x$. On the other hand, a reduction of the drift or even a flux reversal ($\vartheta < 0$) can be induced at larger amplitudes (for small k , according to eq. (20)), while the flux is now found to be an increasing function of the perturbation frequency.

4 Concluding remarks

In conclusion, the rocking ratchet version for Stokes' drift reveals two new features, which are to be attributed to the colour (finite correlation time) of the applied force: the drift is enhanced by small amplitude perturbations, while a flux reversal occurs at sufficiently large amplitude and large correlation time. While our calculations are limited to the case of dichotomic Markov noise, we expect that similar results hold for other coloured noises.

In [5] it was reported that, in two dimensions, both the direction and amplitude of the Stokes' drift can change with the intensity of the Brownian motion when several waves are present. A similar phenomenon will appear here when

one considers, for example, two waves propagating in orthogonal directions x_1 and x_2 . A dichotomic forcing ξ will induce different drifts along these directions depending on its projections $\xi_1 = \pm A_1$ and $\xi_2 = \pm A_2$, as well as on its transition rate k . In particular, by varying k one is able to induce a significant change in the resulting drift direction, as can be seen in fig. 3 for the simple example of identical square waves.

Acknowledgements This work was supported by the Program on Inter-University Attraction Poles of the Belgian Government and the F.W.O. Vlaanderen (CVdB).

References

- [1] G. G. Stokes, *Trans. Camb. Philos. Soc.* **8**, 441 (1847); O. M. Phillips, *The Dynamics of the Upper Ocean*, Cambridge University Press, Cambridge, 1977; J. Lightwill, *Waves in Fluids*, Cambridge University Press, Cambridge, 1978.
- [2] A few recent papers from a rich bibliography on the subject:
A. M. Bratseth, *Tellus* **50A**, 451 (1998); S. M. Cox, *Fluid Dyn. Res.* **19**, 149 (1997); H. C. Graber, B. K. Haus, R. D. Chapman and L. K. Shay, *J. Geophys. Res.* **102**, 18749 (1997) (experimental); J. C. McWilliams, P. P. Sullivan and Chin-Hoh Moeng, *J. Fluid Mech.* **334**, 1 (1997); M. Nordsveen and A. F. Bertelsen, *Int. J. Multiphase Flow* **23**, 503 (1997); V. Polonichko, *J. Geophys. Res.* **102**, 15773 (1997); S. A. Thorpe, *J. Phys. Oceanogr.* **27**, 62 and 2072 (1997).
- [3] See e.g. a recent paper of C. P. Lee, *Phys. of Fluids* **10**, 2765 (1998) and references therein.
- [4] K. Herterich and K. Hasselmann, *J. Phys. Oceanogr.* **12**, 704 (1982); O. N. Mesquita, S. Kane and J. P. Gollub, *Phys. Rev. A* **45**, 3700 (1992).
- [5] K. M. Janson and G. D. Lythe, *Phys. Rev. Lett.* **81**, 3136 (1998); *ibid.*, *J. Stat. Phys.* **90**, 227 (1998).
- [6] C. Van den Broeck, *Europhys. Lett.* **46**, 1 (1999).
- [7] R. Landauer and M. Büttiker, *Physica Scripta* **T9**, 155 (1985).
- [8] M. O. Magnasco, *Phys. Rev. Lett.* **71**, 1477 (1993); M. Bier, *Phys. Lett. A* **211**, 12 (1996); P. Hänggi and R. Bartussek, in *Lect. Notes in Phys.*, vol. **476**, ed. by J. Parisi et al., Springer, Berlin, 1996; R. D. Astumian, *Science* **276**, 917 (1997); F. Julicher, A. Ajdari and J. Prost, *Rev. Mod. Phys.* **69**, 1269 (1997).
- [9] C.R. Doering, W. Horsthemke and J. Riordan, *Phys. Rev. Lett.* **72**, 2984 (1994); K.W. Kehr, K. Mussawisade, T. Wichmann and W. Dieterich, *Phys. Rev. E* **56**, R2351 (1997).
- [10] N. G. Van Kampen, *Stochastic Processes in Physics and Chemistry*, North Holland, Amsterdam, 1981.

- [11] W. Horsthemke and R. Lefever *Noise-Induced Transitions : Theory and Applications in Physics, Chemistry and Biology*, Springer Verlag, 1984.

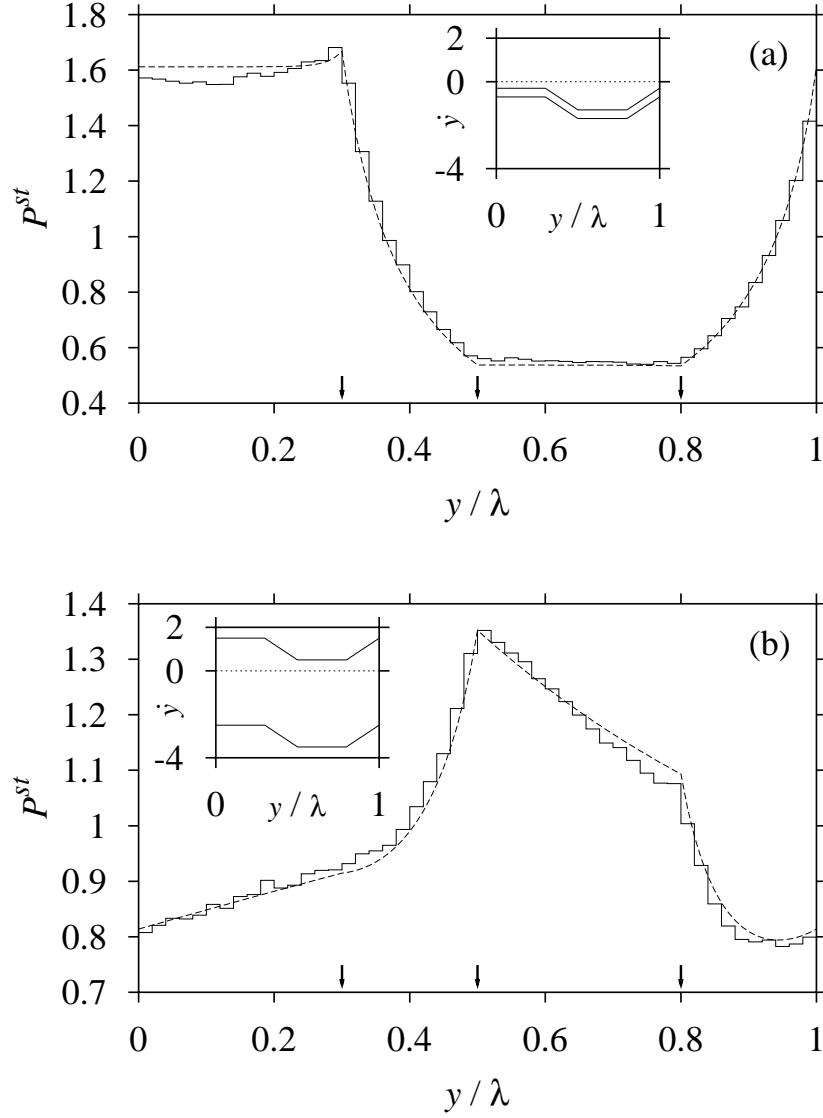


Figure 1: Stationary probability density for the piecewise linear wave, eq. (15), with $v = 1$, $b = 0.5$, $\lambda = 10$ and $\varepsilon = 1$ (the arrows indicate the boundary points of the piecewise linear regions). Dashed lines represent the theoretical results, while solid lines correspond to simulations of 10^6 particles evolving for 200 time units. The insets show the two realisations of \dot{y} . Fig. 1(a): $A = 0.2$, $k = 1$. Fig. 1(b): $A = 2$, $k = 0.1$.

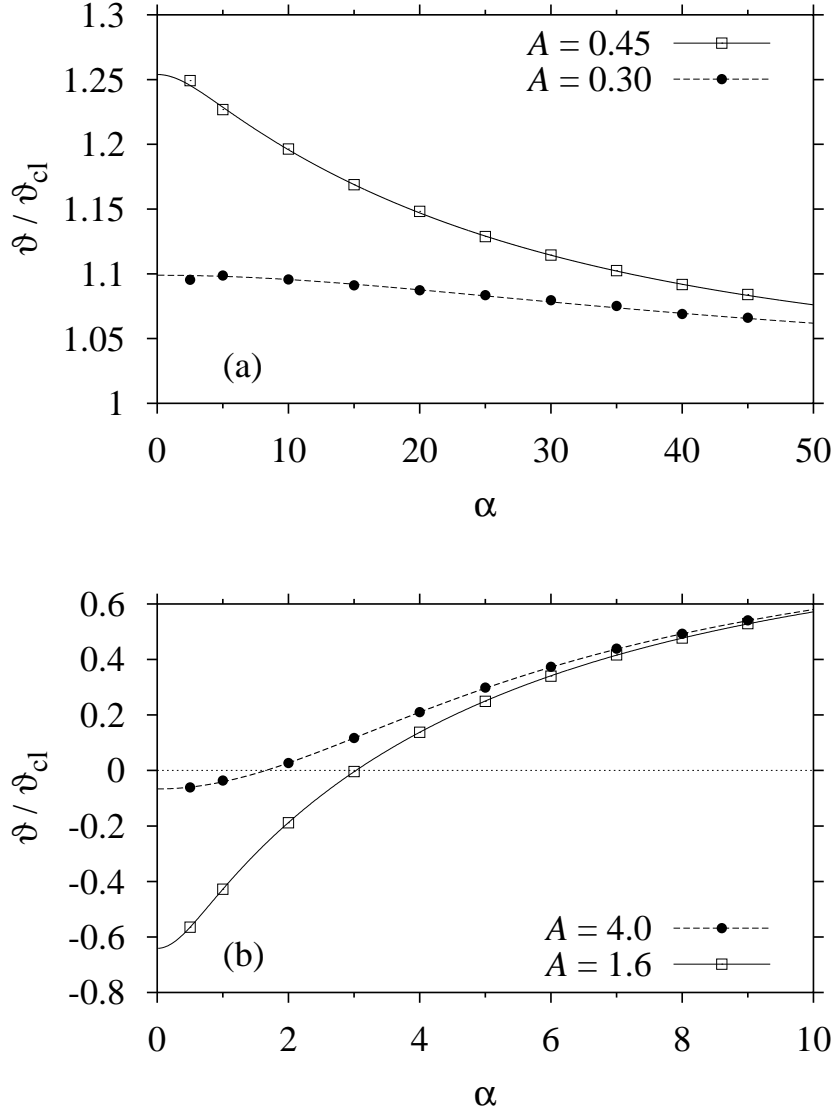


Figure 2: Drift velocity according to eq. (3) for a square wave with the same values of the parameters as in Fig. 1, except here $\varepsilon = 0$. Symbols represent simulations with 10^3 particles measured after 5×10^4 time units. The lines represent the theoretical value, eq. (19). Fig. 2(a): drift enhancement. Fig. 2(b): flux reversal.

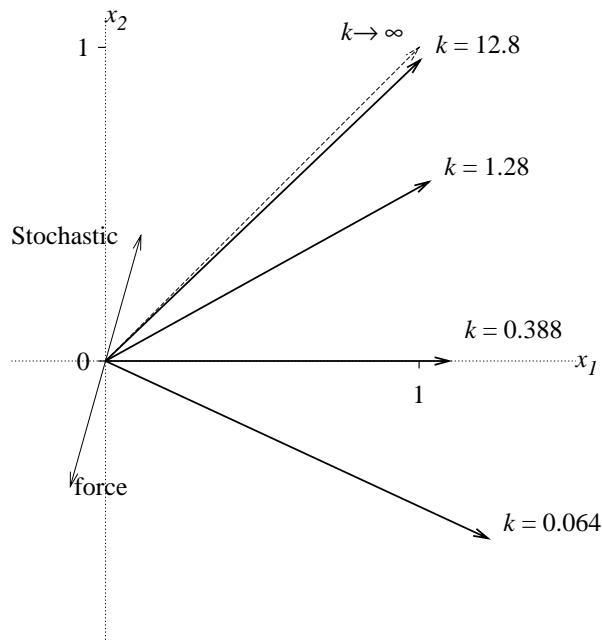


Figure 3: The resulting drift velocity (in units ϑ_{cl} ; thick arrows) for two identical square waves (with the same parameters as in Fig. 1) propagating respectively along the $+x_1$ and $+x_2$ axes, in the presence of a stochastic forcing with $A_1 = 0.45$, $A_2 = 1.6$ (applied along the direction of the thin arrows), for different transition rates k . The dashed arrow corresponds to the classical limit $k \rightarrow \infty$.